Comparative Analysis of Mechanically Induced Long Period Gratings Using Different 3D Printed Grooved Structure Shapes

Sidrish Zahra[a], Elena De Vita[b], Flavio Esposito[c], Agostino Iadicicco[d] and Stefania Campopiano[e]
Department of Engineering, University of Naples "Parthenope", 80143 Naples, Italy

Keywords: 3D Printing, Long Period Gratings, Mechanically Induced Long Period Gratings, Double Cladding Fibers, Photonic Crystal Fibers.

Abstract: This study deals with mechanically induced long period fiber gratings (MILPGs). First, an in-depth analysis of the most effective grating configuration of a grooved structure featuring a duty cycle of 40:60 using SMF-28 is provided. Subsequently, a comparative analysis of MILPGs developed in various multi-layered optical fibers, including double cladding fibers with doped and pure-silica core as well as solid core photonic crystal fiber is presented. The demonstrated fabrication method highlights its adaptability for various types of fibers, eliminating the need for supplementary equipment or modifications, and operates independently of photosensitive fibers which marks the novelty of this work.

1 INTRODUCTION

Optical fiber sensing has attracted much attention due to its high sensitivity, immunity to electromagnetic interference, corrosion resistance, long-distance telemetry, multiplexing, embedding in engineering structures, and distributed measurement (Addanki et al., 2018) and therefore can be used as sensing elements to detect several parameters such as mechanical measurements (Drake et al., 2018), chemical and biological properties (Wolfbeis, 2006; Yin et al., 2018), temperature (Schena et al., 2016), and biomedical parameters (Leal-Junior et al., 2019). Moreover, devices utilizing fiber gratings and especially long period gratings (LPGs) are among the most extensively studied, owing to their diverse applications in optical communication and sensing systems.

The LPG period is large generally tens to hundreds of microns. It can couple the core mode to the cladding modes propagating along the same direction, causing transmission loss of a specific wavelength. LPG has the advantages of extremely low back reflection, full compatibility with optical fiber and low insertion loss. In the field of optical fiber communication, it can be used as a band-stop filter (Vengsarkar et al., 1996), mode converter or grating coupler (Liu et al., 2007); and in the field of optical fiber sensing, it can be used for single parameter or multi-parameter sensing such as temperature, refractive index and bending (Bhatia et al., 1999). Over the past few decades, LPG preparation methods have emerged in an endless stream, rich and diverse. In addition to the very mature UV exposure method (Kalachev et al., 2005), there are also ion beam irradiation method (von Bibra et al., 2001), arc discharge method (Esposito et al., 2019) and so on. The formation mechanisms of these preparation methods are different, which makes the application fields of written LPG also very different.

Every fabrication technique presents unique benefits, yet it is important to acknowledge the inherent limitations as well. For instance, permanent grating can be established using several of the previously mentioned methods. The UV laser technique is limited to photosensitive fiber, and in the

[a] https://orcid.org/0000-0000-4237-7650
[b] https://orcid.org/0000-0003-4975-2775
[c] https://orcid.org/0000-0003-1187-5825
[d] https://orcid.org/0000-0002-3540-7316
[e] https://orcid.org/0000-0002-2987-9122

Zahra, S., De Vita, E., Esposito, F., Iadicicco, A. and Campopiano, S.
Comparative Analysis of Mechanically Induced Long Period Gratings Using Different 3D Printed Grooved Structure Shapes.
DOI: 10.5220/0013400600003902

In *Proceedings of the 13th International Conference on Photonics, Optics and Laser Technology (PHOTOPTICS 2025)*, pages 163-167
ISBN: 978-989-758-736-8; ISSN: 2184-4364

case of the arc discharge method, fiber bending during fabrication could impact real-time monitoring. An alternative technique known as mechanically induced long period grating (MILPGs) exists. Due to the photo-elastic effect, a periodic refractive index modulation is generated at a pressure point on the optical fiber to form a mechanically induced LPG. This method has a simple structure. Since then, MILPG has attracted widespread attention from scholars at home and abroad, and different structures of force-applying devices have been continuously proposed and are widely used in the fields of optical fiber communication and sensing (Lee et al., 2020; Savin et al., 2000), (Rego et al., 2003), (Yokouchi et al., 2005), (Oliveira et al., 2021).

Recently, there has been a growing interest in additive manufacturing technologies for the creation of 3D objects tailored for optical fiber devices (Iezzi et al., 2016). This technology has emerged as the favoured option among the diverse array of available solutions, owing to several appealing characteristics, including affordability, rapid design and production capabilities, on-demand printing, the ability to process polymer materials and, crucially, printing of complex geometries with high resolution (Di Palma et al., 2022).

In this context, this study employed Stereolithography (SLA) 3D printing for the fabrication of mechanically induced long period gratings in different unconventional optical fibers for a specific period of 630 µm. This printing technique not only delivers exceptional detail and surface quality but also enhances material efficiency, as only the resin directly exposed to the light undergoes solidification. The MILPGs are fabricated mainly due to the combined influence of cyclic mechanical strain applied to the fiber generated by the interdigitated 3D printed structure.

2 3D – PRINTING BASED FABRICATION OF MILPG

The fabrication of mechanically induced long-period gratings using 3D printing techniques has become a highly regarded approach in recent years (Oliveira et al., 2021). The creation of MILPGs usually requires the utilization of a 3D-printed structure to generate periodic deformations along the optical fiber, resulting in the formation of the grating pattern. The process starts by creating and printing a unique structure that will be utilized to manipulate the shape of the optical fiber. As the fundamental component of the fabrication process, which causes alteration in the physical or geometrical characteristics of the fiber, is the periodically grooved structure. The process starts by carefully designing 3D CAD (Computer-Aided Design) files. Once the CAD files for 3D model are completed, they are printed using a commercial 3D Anycubic printer. The designing and optimization of grating parameters and their effects have been explained and presented in (Zahra et al., 2023).

The evaluation of the performance of our proposed technique to produce the MILPGs was conducted utilizing the configuration illustrated in Figure 1. The experimental configuration is basic and easy to implement, incorporating a broadband light source alongside an Optical Spectrum Analyzer (OSA) to assess the spectral characteristics of the gratings. To realize the MILPGs, an optical fiber is strategically placed on the base structure (which has a grooved structure in the centre) and subsequently shielded by a cover (has same grooved structure as of base) produced from a 3D printer.

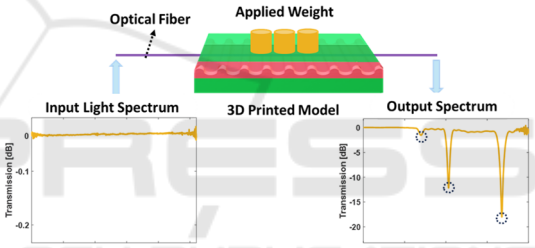

Figure 1: Schematic of Experimental setup for MILPGs.

2.1 Effect of Grating Shape

This study examined the attenuation bands of the MILPGs for two different grating shapes: 1) sinusoidal interdigitated and 2) square shape as depicted in Figure 2. The analysis did not involve removing the external coating of the optical fiber. For this experiment, a sample of externally removed coated standard single mode fiber (SMF-28) was used and tested for a period of 660 µm (as an example) with an optimized grating length of 39.5 mm.

For our initial approach, we utilized a square interdigitated grating style with a duty cycle of 40:60. This design involved creating grooved structures on both the base and cover of a 3D object for MILPG. During the design and testing process, a square shape with interdigitated features was observed to exhibit two attenuation bands at specific wavelengths as can be seen in Figure 3. These bands, referred to as λ_1 and λ_2, were located at 1577.4 nm and 1633.6 nm, respectively. The depth of attenuation for λ_1 was

measured at 15.7 dB, while λ_2 had a depth of 16.7 dB. These results were obtained using an applied weight of 1614 g.

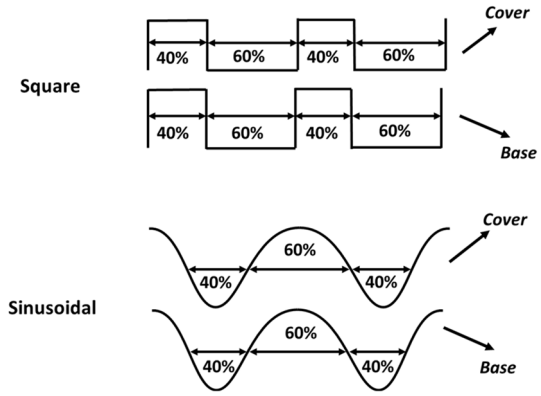

Figure 2: Schematic of interdigitated sinusoidal and square geometry for our MILPFGs using SMF-28 (660 µm).

In the next attempt, a sinusoidal interdigitated grating shape was designed and tested. The results revealed the presence of two attenuation bands, one at 1635.6 nm and another at 1578.4 nm. These bands exhibited depths of 27.9 dB and 16 dB respectively, when an applied weight of 1735 g was used.

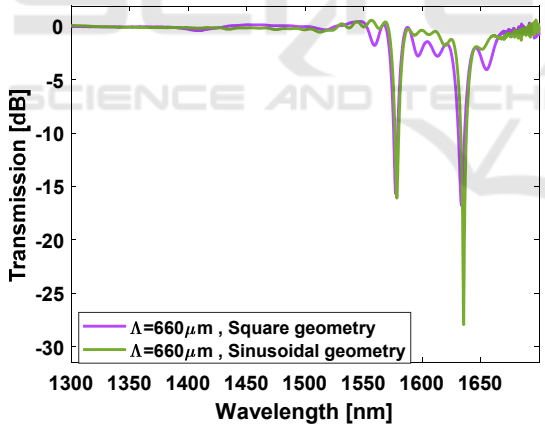

Figure 3: Comparison of interdigitated sinusoidal and square geometry for our MILPFGs using SMF-28 (660 µm).

When comparing these two distinct shapes, it is interesting to note that both produced attenuation bands located at similar wavelengths, but the sinusoidal interdigitated grating style showed a remarkably high depth of attenuation bands. Additionally, the sinusoidal interdigitated shape had narrower attenuation bands with fewer ripples compared to the square interdigitated shape, as presented in Figure 3. This feature makes it the perfect option for creating MILPGs in optical fiber for future applications.

2.2 MILPGs in Unconventional Fibers

Starting from the results reported in the previous section about the shape of grooved structure, we evaluate the versatility of fabricating MILPGs by selecting a period of 630 µm (and optimized grating length of 37.4 mm), for different types of multi-layered unconventional optical fibers including i) Thorlabs DCF-13 progressively three-layered double cladding fiber (DCF); ii) pure-silica core Nufern S1310 DCF with W-type structure; iii) NKT ESM-12-01 solid core pure-silica photonic crystal fiber (PCF). The DCF-13 represents a commercially available double cladding fiber meticulously developed to facilitate both single-mode and multi-mode operation via its core and the very first cladding. It has core diameter D_{co} equal to 9 µm and an inner cladding with diameter $D_{cl,in}$ equal to 105 µm while the outer cladding has a diameter of $D_{cl,out}$ equal to 125 µm. Like DCF-13, the Nufern S1310 has three concentric layers: core, inner cladding, and outer cladding. The fibre has a 9 µm diameter core made of pure silica. The inner cladding, doped with fluorine, has a diameter of 95 µm, while the outside cladding, constructed of pure silica, has a diameter of 125 µm.

Moreover, a PCF was considered with a solid core region with a diameter of 12 µm, while the cladding region with a diameter of 60 µm is micro-structured with periodic air holes.

The test used the identical experimental setup presented in Figure 1. The preliminary evaluation of the mechanically induced long period grating focused on assessing its compatibility with unconventional fibers. This investigation provides a concise overview of the fabrication process of MILPGs implemented for the 630 µm period, specifically for DCF-13 fiber.

Figure 4 illustrates the evolution of the transmission spectra as the applied weight was systematically increased from 860 g to 1250 g. As it can be seen from the Figure 4 that weights below 860 g created insignificant transmission spectra attenuation regions. As weight reached a specific value, attenuation bands got more noticeable, reaching up to 7 dB. Additional weight increased depth to 15 dB at 1250 g. Even though not indicated here, over-coupling reduces attenuation band depth as the applied weight exceeds 1250 g. According to LPG operating concept, the depth of the attenuation band grows with modulation intensity (in this case applied weight) until it reaches a maximum value, then drops. The results showed three attenuation bands at 1636,

1506, and 1439 nm. The bands had maximum depths of 15 dB, 11 dB, and 1 dB, respectively, due to the interaction between the core mode and the 3rd, 2nd, and 1st order cladding modes (λ_3, λ_2, and λ_1). It can be noticed that the intensity of mode coupling increases with weight, resulting in a stronger resonance (Figure 4). Weight affects attenuation band intensification, but resonant wavelengths remain fixed and ultimately peak progression is precisely managed using this attribute.

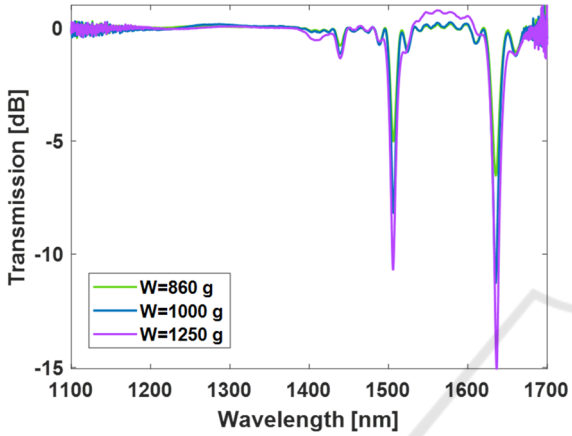

Figure 4: Transmission spectra of DCF-13 for 630 µm with an optimized grating length of 37.8 mm.

The same procedure was followed for the rest of the reported optical fibers and their measured spectra are presented in Figure 5, where it can be seen that when Nufern S1310 fiber was tested, two attenuation bands were found at 1547 nm (λ_3) and 1449 nm (λ_2), with maximum depths of 19 dB and 20 dB, respectively, with 1614 g of weight applied. It can be concluded that the utilization of DCF-13 allows for the generation of attenuation bands with maximum depth while requiring a reduced amount of applied weight. Nufern fiber exhibits a slightly greater depth for the attenuation band compared to DCF-13, however with an increased weight relative to DCF-13.

The same LPG period of 630 µm used in DCF-13 and Nufern S1310 was used to study grating generation in photonic crystal fibre. As the experimental setup shows that weight on the 3D printed structure symmetrically distributes mechanical stress. This microbending of the fiber in the grooved structure deforms the air hole structure of the PCF which ultimately changes the refractive index and helps core-cladding coupling. The acquired MILPG transmission spectra in PCF is illustrated in Figure 5. The attenuation band is clearly observed at a wavelength of 1230 nm, exhibiting a depth of 14 dB

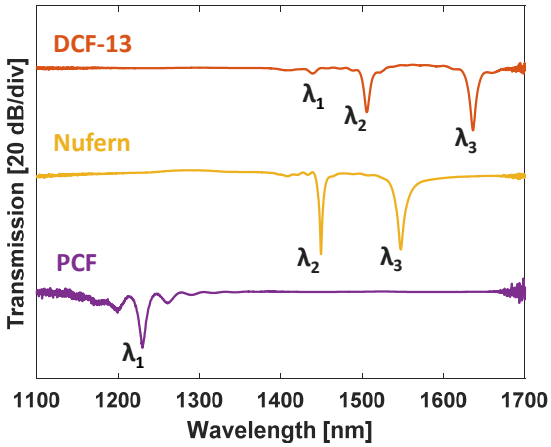

Figure 5: Transmission spectra of different fibers for 630 µm period with an optimized grating length of 37.8 mm.

when an applied weight of only 790 g was utilized. For photonic crystal fibres, the potential to achieve attenuation bands with significant depth is realised, although these bands may be broader compared to those found in DCF-13 and Nufern S1310. In conclusion, it is observed that for DCF-13 and Nufern S1310, coupling was successfully achieved up to the third order cladding mode. In contrast, for PCF, coupling was limited to the first order over a distance of 630 µm, which may influence aspects such as sensing performance, explained in detail in (Zahra et al., 2024)

3 CONCLUSION

The present study details the innovative fabrication of mechanically induced long period gratings within diverse multi-layered silica fibers, including two varieties of double cladding fibers (featuring progressively three-layered and W-type structures) and solid core photonic crystal fiber, utilizing a 3D printing technique for the first time in accordance with the latest advancements in the field. A concise examination of the fabrication of MILPGs was performed for the aforementioned fibers, and their transmitted spectra were evaluated within the wavelength range of 1100-1700 nm. The devices demonstrate remarkable spectral properties, featuring low power losses, precise depth, and narrow attenuation bands, achieved through an easy and economical approach. The findings highlight the adaptability of our proposed technology, which works irrespective of photosensitive fibers. This capability enables its application to various types of fibers

without the need for supplementary equipment or modifications.

REFERENCES

Addanki, S., Amiri, I. S., & Yupapin, P. (2018). Review of optical fibers-introduction and applications in fiber lasers. *Results in Physics*, 10, 743–750. https://doi.org/10.1016/j.rinp.2018.07.028

Bhatia, V., Glenn, W. H., Farina, J. D., Leonberger, F. J., Vengsarkar, A. M., Lemaire, P. J., Judkins, J. B., Bhatia, V., Sipe, J. E., & Ergodan, T. E. (1999). Applications of long-period gratings to single and multi-parameter sensing. *OPTICS EXPRESS*, 4, 225. https://doi.org/10.1364/OA_License_v1#VOR

Di Palma, P., De Vita, E., Iadicicco, A., & Campopiano, S. (2022). 3D Shape Sensing With FBG-Based Patch: From the Idea to the Device. *IEEE Sensors Journal*, 22, 1338–1345. https://doi.org/10.1109/JSEN.2021.3133704

Drake, D. A., Sullivan, R. W., & Wilson, J. C. (2018). Distributed strain sensing from different optical fiber configurations. *Inventions*, 3(4). https://doi.org/10.3390/inventions3040067

Esposito, F., Srivastava, A., Campopiano, S., & Iadicicco, A. (2019). Sensing Features of Arc-induced Long Period *Gratings*. 29. https://doi.org/10.3390/proceedings2019015029

Iezzi, V. L., Boisvert, J.-S., Loranger, S., & Kashyap, R. (2016). 3D printed long period gratings for optical fibers. *Optics Letters*, 41(8), 1865. https://doi.org/10.1364/ol.41.001865

Kalachev, A. I., Pureur, V., & Nikogosyan, D. N. (2005). Long-period fiber grating inscription by high-intensity femtosecond UV laser pulses. *Quantum Electronics and Laser Science Conference* (QELS), 2, 951–953. https://doi.org/10.1109/qels.2005.1548993

Leal-Junior, A. G., Diaz, C. A. R., Avellar, L. M., Pontes, M. J., Marques, C., & Frizera, A. (2019). Polymer optical fiber sensors in healthcare applications: A comprehensive review. In *Sensors (Switzerland)* (Vol. 19, Issue 14). MDPI AG. https://doi.org/10.3390/s19143156

Lee, J., Kim, Y., & Lee, J. H. (2020). A 3-D-printed, temperature sensor based on mechanically-induced long period fibre gratings. *Journal of Modern Optics*, 67(5), 469–474. https://doi.org/10.1080/09500340.2020.1737741

Liu, Y., Chiang, K. S., Rao, Y. J., Ran, Z. L., & Zhu, T. (2007). Light coupling between two parallel CO2-laser written long-period fiber gratings. *Opt. Express*, 15(26), 17645–17651. https://doi.org/10.1364/OE.15.017645

Oliveira, R., Sousa, L. M., Rocha, A. M., Nogueira, R., & Bilro, L. (2021). Uv inscription and pressure induced long-period gratings through 3d printed amplitude masks. *Sensors*, 21(6), 1–14. https://doi.org/10.3390/s21061977

Rego, G., Fernandes, J. R. A., Santos, J. L., Salgado, H. M., & Marques, P. V. S. (2003). New technique to mechanically induce long-period fibre gratings. *Optics Communications*, 220(1–3), 111–118. https://doi.org/10.1016/S0030-4018(03)01374-9

Savin, S., Digonnet, M. J. F., Kino, G. S., & Shaw, H. J. (2000). Tunable mechanically induced long-period fiber gratings. *Optics Letters*, 25(10), 710. https://doi.org/10.1364/OL.25.000710

Schena, E., Tosi, D., Saccomandi, P., Lewis, E., & Kim, T. (2016). Fiber Optic Sensors for Temperature Monitoring during Thermal Treatments: An Overview. *Sensors (Basel, Switzerland),* 16. https://api.semanticscholar.org/CorpusID:4964243

Vengsarkar, A. M., Lemaire, P. J., Judkins, J. B., Bhatia, V., Erdogan, T., & Sipe, J. E. (1996). Long-period fiber gratings as band-rejection filters. *Journal of Lightwave Technology,* 14(1), 58–64. https://doi.org/10.1109/50.476137

von Bibra, M. L., Roberts, A., & Canning, J. (2001). Fabrication of long-period fiber gratings by use of focused ion-beam irradiation. *Opt. Lett.,* 26(11), 765–767. https://doi.org/10.1364/OL.26.000765

Wolfbeis, O. S. (2006). Fiber-Optic Chemical Sensors and Biosensors. *Analytical Chemistry*, 78(12), 3859–3874. https://doi.org/10.1021/ac060490z

Yin, M., Gu, B., An, Q.-F., Yang, C., Guan, Y. L., & Yong, K.-T. (2018). Recent development of fiber-optic chemical sensors and biosensors: Mechanisms, materials, micro/nano-fabrications and applications. *Coordination Chemistry Reviews*, 376, 348–392. https://doi.org/https://doi.org/10.1016/j.ccr.2018.08.001

Yokouchi, T., Suzaki, Y., Nakagawa, K., Yamauchi, M., Kimura, M., Mizutani, Y., Kimura, S., & Ejima, S. (2005). Thermal tuning of mechanically induced long-period fiber grating. *Applied Optics*, 44(24), 5024. https://doi.org/10.1364/AO.44.005024

Zahra, S., De Vita, E., Esposito, F., Iadicicco, A., & Campopiano, S. (2024). Mechanically induced long period gratings in different silica multi-layered optical fibers. *Optical Fiber Technology*, 85. https://doi.org/10.1016/j.yofte.2024.103814

Zahra, S., Di Palma, P., De Vita, E., Esposito, F., Iadicicco, A., & Campopiano, S. (2023). Investigation of mechanically induced long period grating by 3-D printed periodic grooved plates. *Optics and Laser Technology*, 167. https://doi.org/10.1016/j.optlastec.2023.109752